Supplementary Figures 1-5

Li *et al*,

Polymerase-Mediated Ultramutagenesis in Mice Produces Diverse Cancers with High Mutational Load

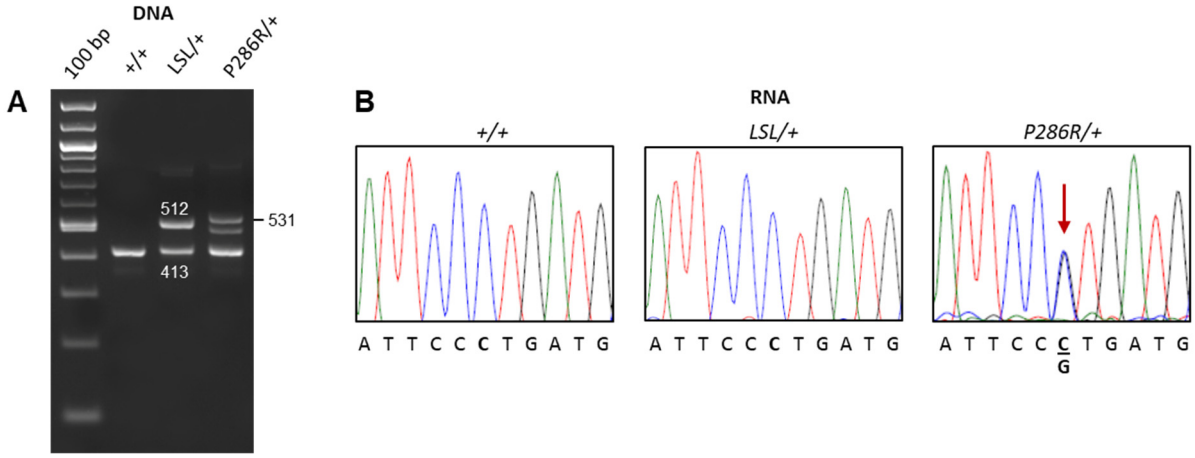

Supplementary Fig. 1. Molecular validation of allele function. A) Multiplex genotyping protocol (tail DNA) distinguished between *+* (wt), *LSL* (*LSL-Pole*^{P286R}), and *P286R* (*Pole*^{P286R}) alleles. Product sizes (bp) are shown. The *P286R* product typically appears as a doublet but this does not affect interpretation of genotyping. B) RT-PCR using intron-spanning primers to characterize allele expression at RNA level. There is no expression from the *LSL* allele, as expected, whereas the *P286R* and wild-type alleles result in equal expression at that RNA level.

A

500 cells regular media ⇩ | 10^6 cells, 60µM 6-TG ⇩

	plating efficency		6-TG resistant colonies	
	P286R/+	*+/+*	*P286R/+*	*+/+*
	140	124	7	0
	131	129	10	0
	142	115	9	0
	138	130	5	0
	120	126	8	0
mean	134	125	7.8	0

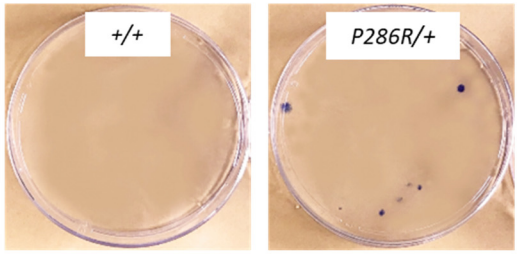

Observed *HPRT1* mutation frequency:
+/+ : 0
P286R/+ : 2.9×10^{-5}
P value, unpaired T test: *p<0.0001*

B

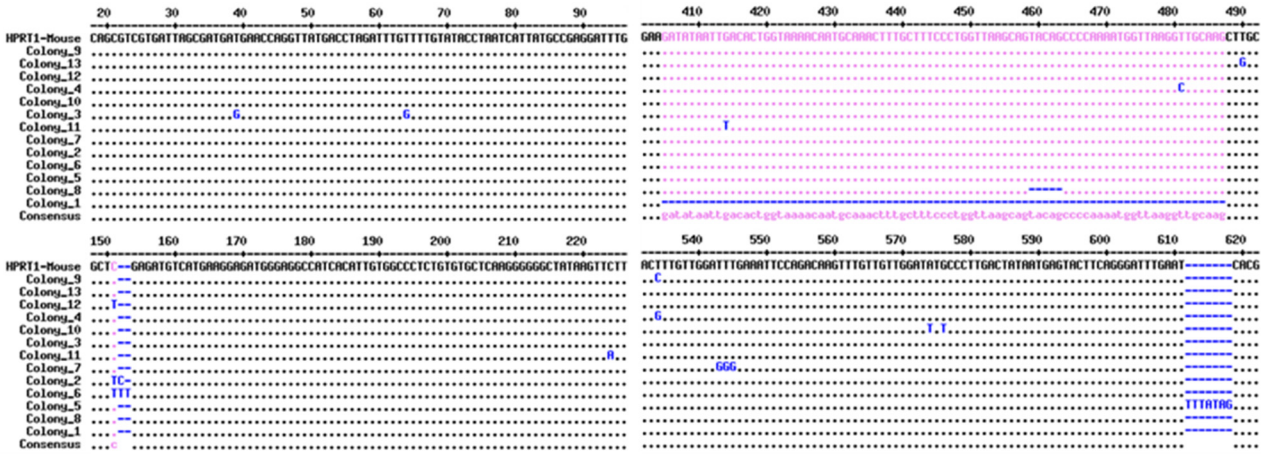

Supplementary Fig. 2. 6-TG selection of passage 20 MEFs. A) Plating efficiency and resistant colonies. Each row represents a separate plate (selection of 10^6 cells). B) cDNA sequencing of *HPRT* locus reveals mutations in each of 13 independent 6-TG resistant colonies; most are nonsynonymous substitutions. Only regions of the cDNA with mutations are shown.

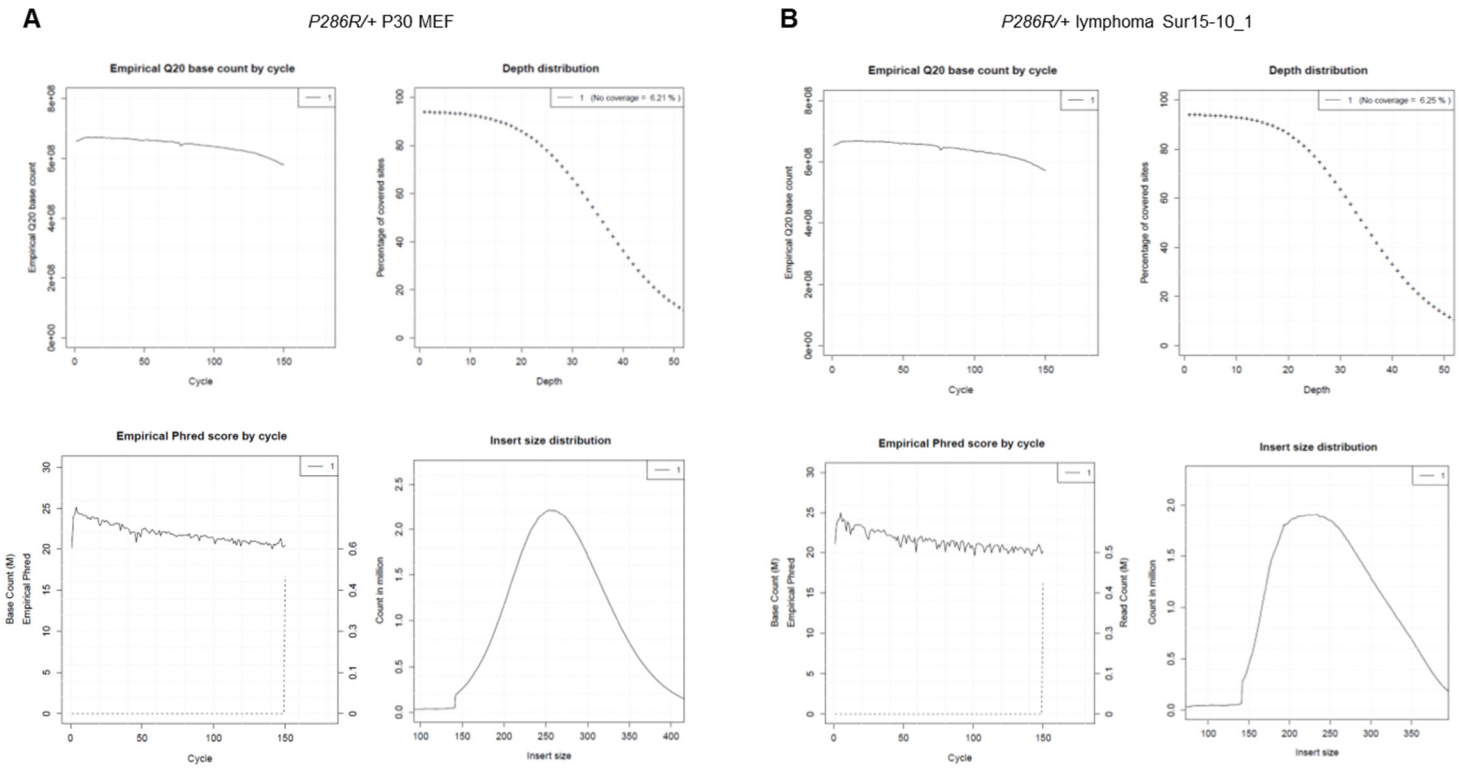

Supplementary Fig. 3. General quality control metrics of WGS data. Representative analyses are provided for two of the samples; metrics were comparable across all samples.

Supplementary Fig. 4. Copy number plots from WGS data (individual samples). For each sample the y-axis represents the normalized depth (log2(depth/median depth across genome)). The x-axis represents the position among the 19 autosomes as illustrated in the legend. The analysis shows that *Pole*^{P286R} does not result in large-scale chromosomal copy-number instability. A) Parental mouse strains. B) Representative passage 30 MEF line clones. Some rearrangements occur during passaging of MEFs but these are qualitatively the same among wild-type and mutant MEFs. C) Tumors from *Pole*^{P286R}*/+* mice. D) Tumors from *Pole*$^{P286R/LSL}$ (hemizygous) mice.

Supplementary Figure 5.

***P286R/+* MEF line clones**

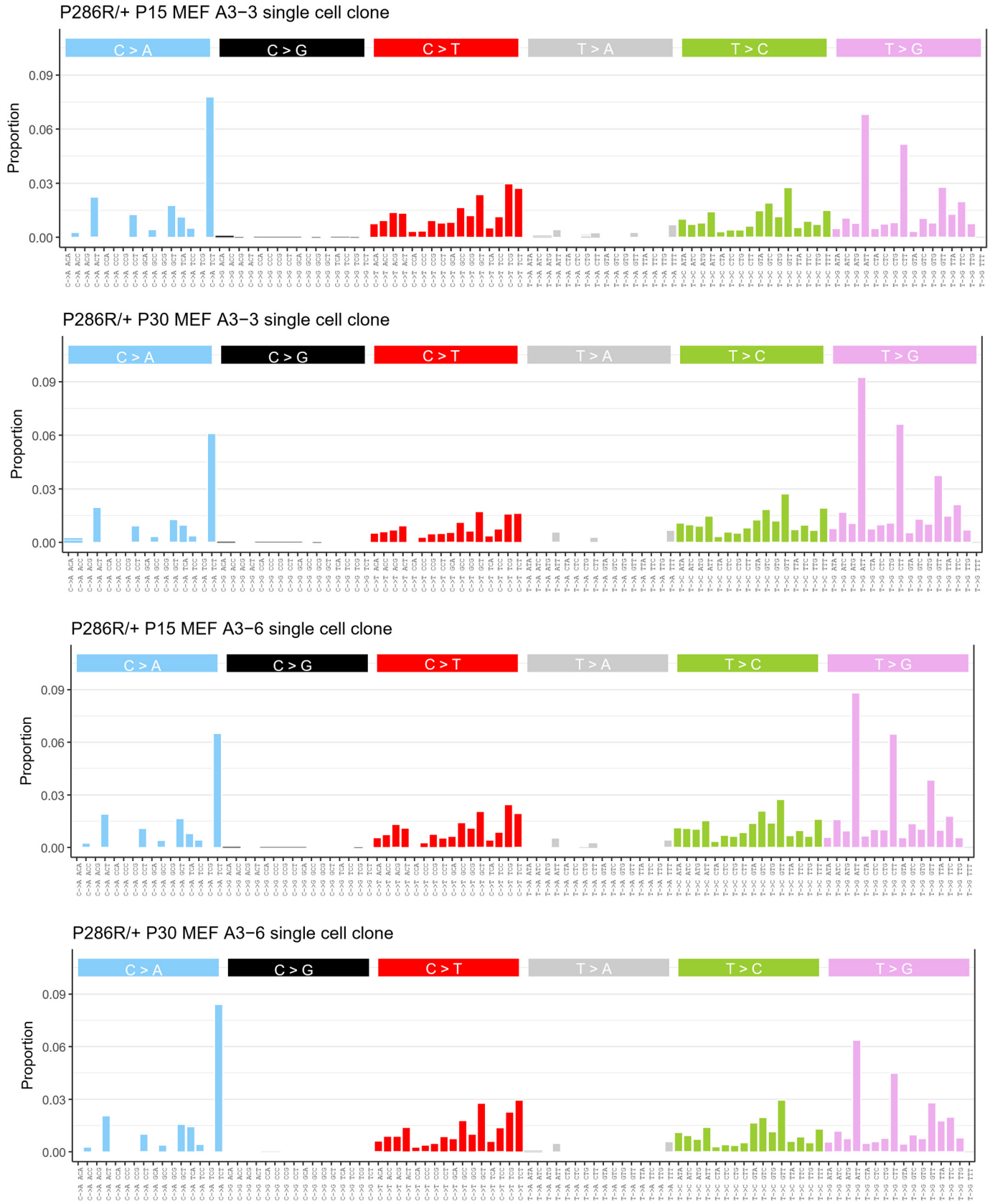

Supplementary Fig. 5

P286R/+ MEF line clones *continued*

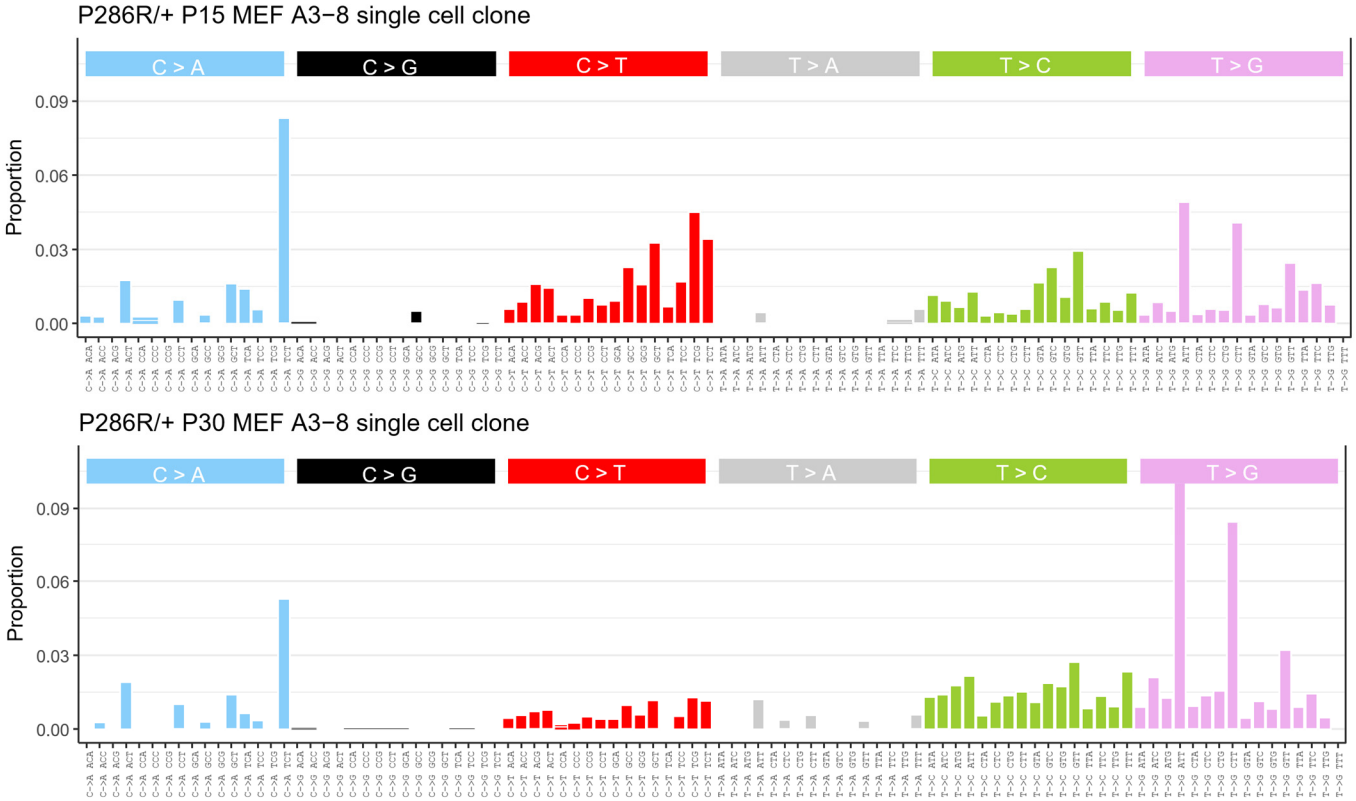

P286R/LSL (hemizygous) tumors

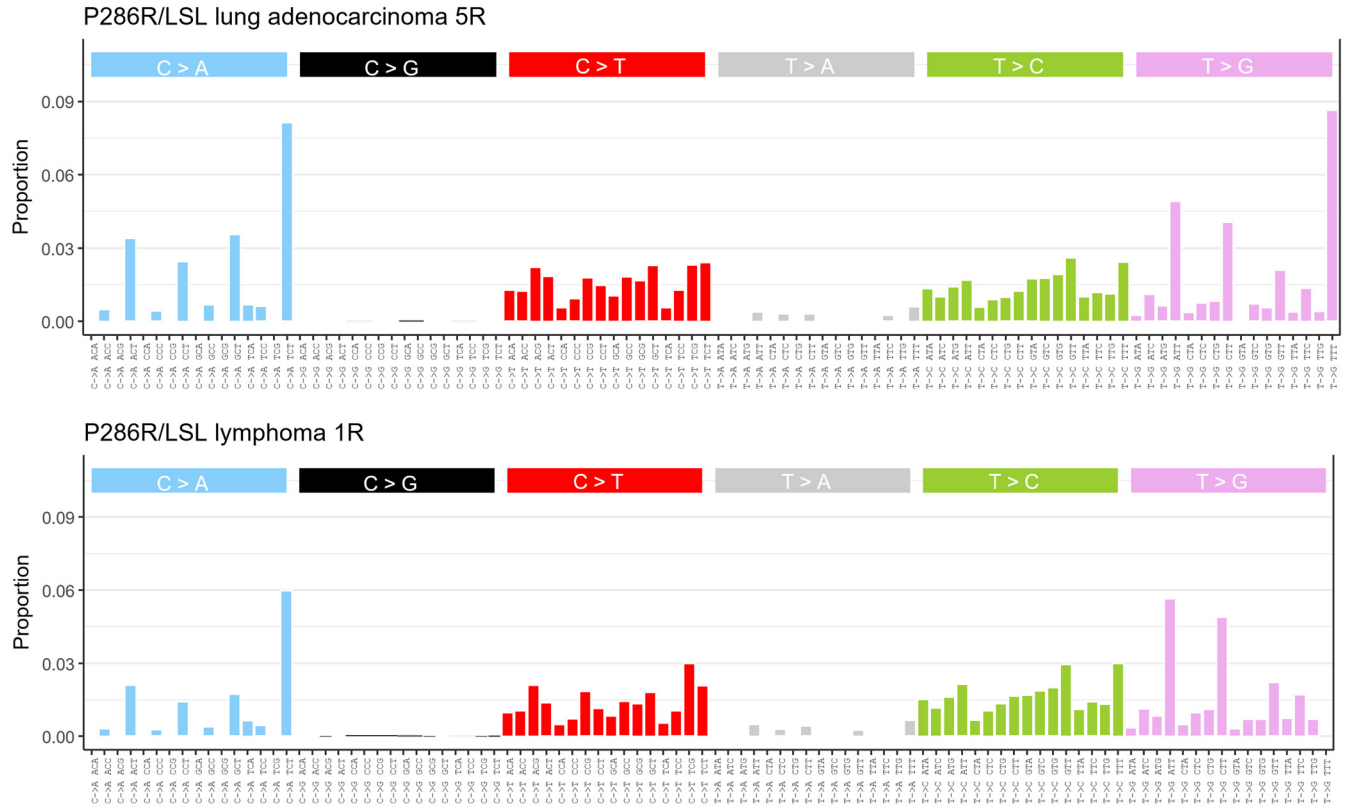

Supplementary Fig. 5

P286R/LSL* (hemizygous) tumors *continued

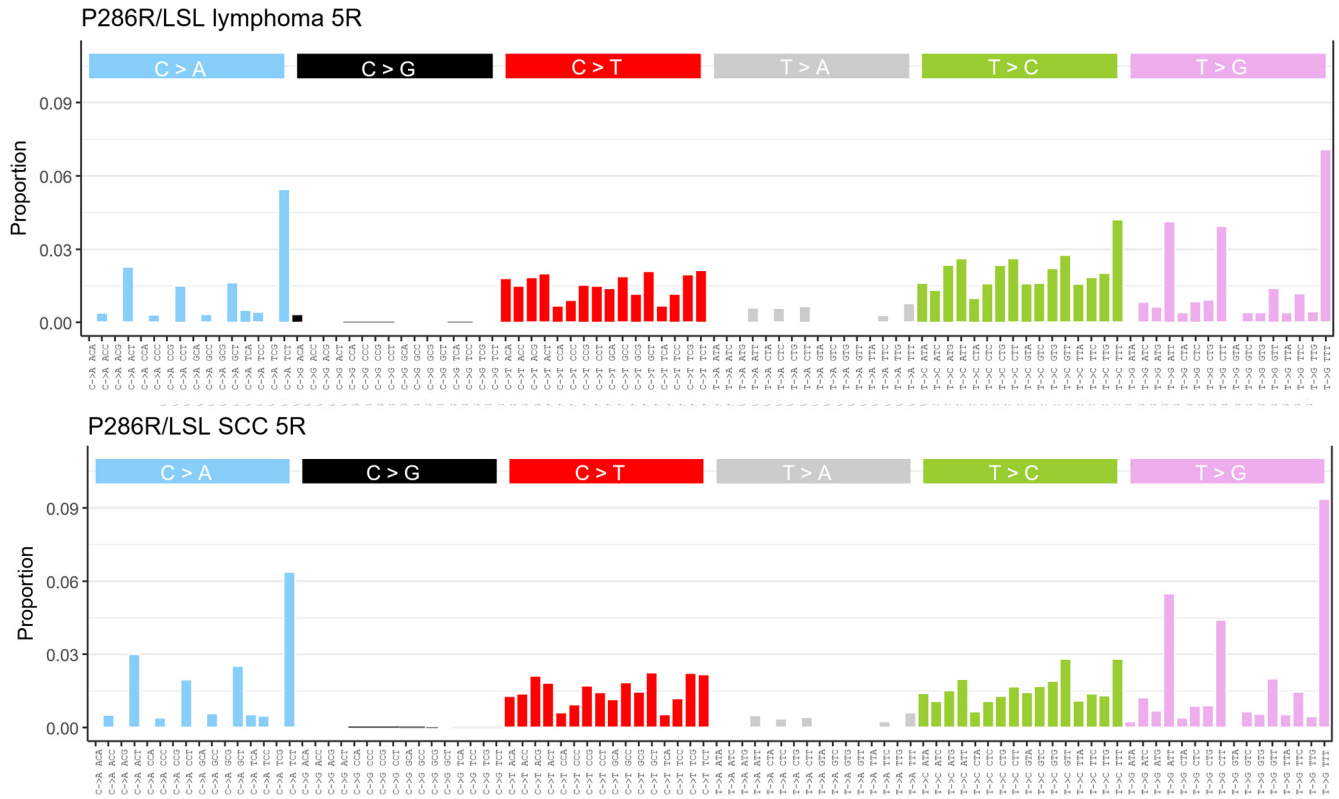

***+/+* MEF line clones**

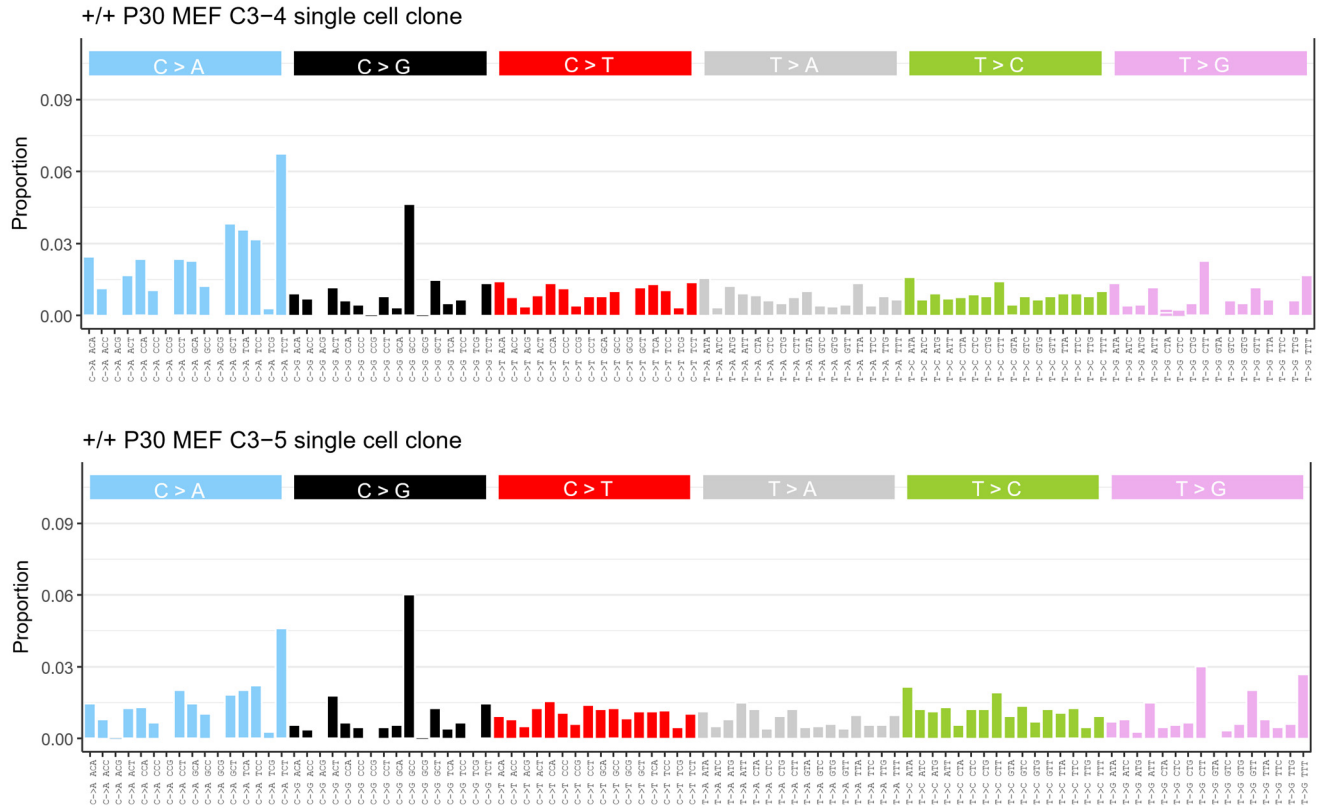

Supplementary Fig. 5

+/+* MEF line clones *continued

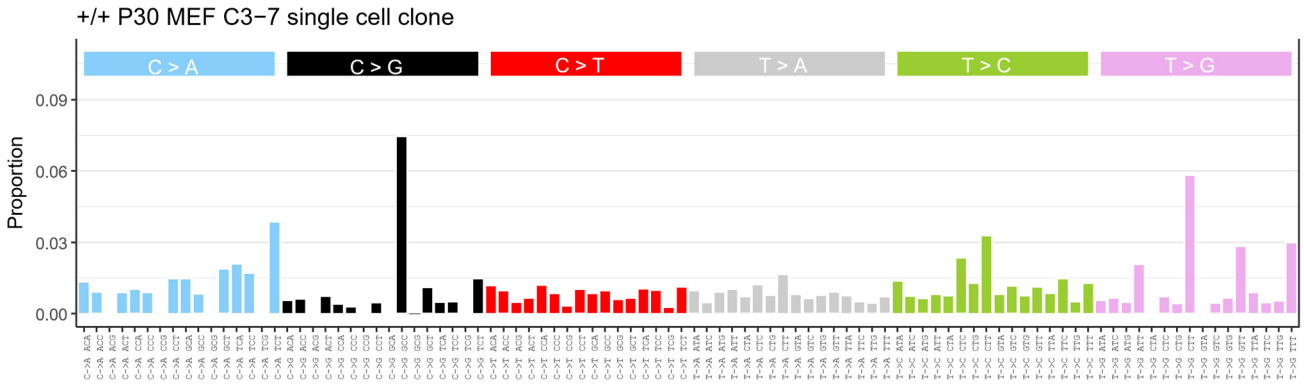

Supplementary Fig. 5. Whole genome sequencing-derived mutational signatures in *Pole*^{P286R}*/+* (heterozygous) MEFs and tumors, and (hemizygous) *Pole*$^{P286R/LSL}$ tumors, and wild-type (*+/+*) MEFs. The 96 possible mutation types based on trinucleotide context are shown for each sample that underwent WGS in this study.